ARCHIVES
of
FOUNDRY ENGINEERING

ISSN (2299-2944)
Volume 2025
Issue 2/2025

69 – 73

9/2

10.24425/afe.2025.153796

Published quarterly as the organ of the Foundry Commission of the Polish Academy of Sciences

Phase Transformations of Siderite in Different Atmospheres - Mössbauer Spectroscopy Study

M. Kądziołka-Gawel [a, *], Z. Adamczyk [b], M. Wojtyniak [b], J. Klimontko [a], J. Nowak [b]
[a] University of Silesia, Poland
[b] Silesian University of Technology, Poland
* Corresponding author: e-mail: mariola.kadziolka-gawel@us.edu.pl

Received 30.09.24; accepted in revised form 31.01.25; available online 13.06.2025

Abstract

The decomposition process of siderite ($FeCO_3$) heated in an oxygen atmosphere and in a vacuum up to a temperature of 700 °C, and the identification of the products of this process was studied using the ^{57}Fe Mössbauer spectroscopy method. Two siderite samples were used for investigations. The measurements showed that one of the siderites was pure $FeCO_3$, and the other had significant amounts of magnesium $(Fe,Mg)CO_3$. The research results indicate that the siderite decomposition process begins at a temperature of 300 °C. The main products of siderite decomposition are Fe-oxide nanoparticles. The crystallization process of these Fe-oxide begins at temperatures at which the decomposition of siderite almost ends, i.e., around 400 °C for $FeCO_3$ and 500 °C for $(Fe,Mg)CO_3$. The final products of siderite decomposition are hematite and magnetite or magnesioferrite. The magnetite formed in this process is poorly crystalline, what is confirmed by X-ray diffraction measurements and the shape of the Mössbauer spectra.

Keywords: Siderite, Fe-oxides, Thermal decomposition, Mössbauer spectroscopy

1. Introduction

Iron is the fourth most abundant element in the Earth's crust. In terms of mineralogy, iron formations are composed of carbonates, silicates, sulfides, and hydroxides, commonly occurring in variable combinations [1]. The presence of carbonates in the Earth's interior is related to the subduction process, one of the first steps in cycling carbon through the Earth [2]. The most common iron carbonate is siderite ($FeCO_3$), a frequent constituent of carbonate sediments and rocks on Earth. The theoretical Fe content in this mineral is 48.27 %wt [3], but natural siderites often contain significant Mg, Ca, and Mn substitutions for Fe in the lattice, and pure siderite is seldom found.

The thermal decomposition of siderite in various atmospheres is widely used for multiple applications, and the products resulting from this process are also significant. This carbonate is one of the primary sources of iron in Europe, in petroleum drilling fluids as a scavenger for H_2S and in processes for making ferrous catalyst materials [4, 5] or in the combustion of the coast [6]. Thermal decomposition characteristics of siderite are utilized in paleomagnetic studies, where the transformation of siderite into magnetite and maghemite can potentially carry a chemical remanent magnetization [7]. The topic of siderite decomposition and oxidation is very interesting because of its commercial importance and related scientific issues connected to the products of this process. Owing to the poor thermal stability, this iron carbonate can decompose into different iron oxides depending on the thermal treatment. Identification of decomposition products of

natural siderite is difficult due to the significant amount of Fe substitution in the lattice by Mg, Ca, and Mn [8]. The final products of the thermal decomposition of siderite are generally hematite in an oxidizing atmosphere, magnetite in a carbon dioxide atmosphere, and magnetite and wustite in an inert atmosphere or a vacuum [7, 9].

This work investigated the mechanism of siderite's thermal decomposition in an air and a vacuum atmosphere. Phase identification was characterized by ^{57}Fe Mössbauer spectroscopy and X-ray diffraction (XRD). Identifying phases formed during the siderite annealing process complements many studies in which we obtain only information about the final products. Additionally, such research can have profound implications, for example, in the processing of siderite ore through a combination of metallurgy and dressing or in the study of the properties and kinetics of its decomposition to better understand the technology of magnetizing roasting of lump siderite ore.

2. Materials and Methods

The studied siderites come from the Ruda coal seams' upper parts, in the Chwałowice Trough's eastern part, in the Upper Silesian Coal Basin. The research was carried out on two rock samples taken from different seams. These samples were designated Sd1 and Sd3. Siderite samples were heated in an air and a vacuum atmosphere from room temperature to 700 ºC for one hour. After heating at a given temperature (300 ºC, 350 ºC, 400 ºC, 450 ºC, 500 ºC, 550 ºC, 600 ºC, 700 ºC) Mössbauer measurements and XRD (for selected temperatures) measurements were performed.

The chemical composition of the investigated samples was determined by X-ray fluorescence (XRF) with a ZSX Primus II Rigaku spectrometer. The spectrometer, equipped with the 4 kW, 60 kV Rh anode and wavelength dispersion detection system, allowed for the analysis of the elements from Be to U. The samples for the study were prepared in the form of pressed tablets.

Minerals present in the investigated raw siderite samples and after annealing at 700 ºC in an air and a vacuum were determined using the X-ray diffraction method. These studies were conducted at room temperature using a Siemens D5000 X-ray diffractometer and CuKα radiation. Rietveld refinement was performed in a licensed X'Pert High Score Plus with a PDF-4 crystallography database. The percentages of individual components in initial samples were determined using the Rietveld method.

The ^{57}Fe Mössbauer transmission spectra were recorded at room temperature using an Integrated Mössbauer Spectroscopy Measurement System (designed by Wacław Musiał and Jacek Marzec), and a linear arrangement of source ^{57}Co:Rh, a multichannel analyzer, an absorber, and a detector. Spectrometer velocity scale was calibrated at room temperature with a 25 μm thick α-Fe foil. The Mössbauer spectra were evaluated by least-square fitting of the lines using the MossWinn4.0i program. Some parts of the spectra were fitted with a hyperfine magnetic field distribution. The model and implementation are based on the Voigt-based fitting method [10].

3. Result and Discussion

X-ray diffraction measurements showed that the initial siderite samples contained siderite ($FeCO_3$) as the main component and small amounts of accompanying minerals such as quartz (SiO_2), illite ($K_{0.65}Al_{2.0}[Al_{0.65}Si_{3.35}O_{10}](OH)_2$), dolomite $CaMg(CO_3)_2$, and kaolinite ($Al_2Si_2O_5(OH)_4$) (Table 1, Figure 1). The annealed samples contained hematite (α-Fe_2O_3) and magnetite (Fe_3O_4) as the only iron phases, with hematite dominating the Sd1 sample and magnetite in the Sd3 sample. Moreover, in the case of the Sd3 sample, a line shift into higher angles compared to pure magnetite is visible, indicating a significant defect in this structure by Mg [11]. In the case of this sample, we can talk about magnesioferrite rather than magnetite. The heated samples also contained significant amounts of quartz, probably due to the sample's high-temperature decomposition of other minerals. Additionally, much of the heated material was amorphous (Table 1). The diffraction lines associated with magnetite (Sd1 sample) or magnesioferrite (Sd3 sample) are significantly broadened (Figure 1). Therefore, the amorphous substance will be mainly related to these poorly crystalline iron oxides. It should also be noted that with such a high content of amorphous substance, quantitative Rietveld phase analysis for phases with contents slightly higher than 1.0 %wt gives these contributions with relative errors even higher than 20 % [12]. However, such phases cannot be omitted in the fitting procedure because the diffraction lines are visible in the diffractograms.

Table 1.
Mineral composition of investigated initial and annealed at 700 ºC in an air and a vacuum siderite samples (Sd1 and Sd3) based on XRD analyses by the Rietveld method in vol. %

Component	**Sd1**		**Sd3**	
	Initial sample			
Siderite	94		84	
Quartz	Trace		7	
Illite	Trace		3	
Dolomite	Trace		Trace	
Kaolinite	5		6	
sum	*99*		*100*	
Component	**Annealed at 700 ºC**			
	Air	**Vacuum**	**Air**	**Vacuum**
Hematite	69	21	6	6
Quartz	2	6	8	4
Magnetite	2	-	-	-
Magnesioferrite	-	-	33	19
Amorphous substance	27	73	53	71
sum	*100*	*100*	*100*	*100*

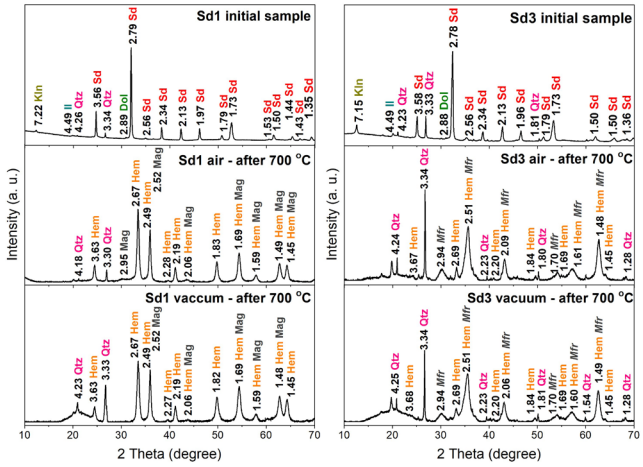

Fig. 1. XRD patterns of the initial and heated at 700 ºC in an air atmosphere and a vacuum siderite samples (Sd1 and Sd3). The main interplanar spacing values are shown in the diffractograms. Sd - siderite, Kln - kaolinite, Il – illite, Dol – dolomite, Mag - magnetite, Mfr -magnesioferrite, Hem - hematite, Qtz - quartz

Table 2 presents the contents of the elements in the investigated raw siderite samples. These data concern elements whose concentration in the sample was higher than 0.5 %wt. Large amounts of Fe, Si, and Al, just as C and O, are elements of minerals present in rock siderite samples (Table 1). It should be noted that the investigated samples also contain small amounts of Ca and Mg. The latter element occurs in relatively large quantities in the Sd3 sample. The large amount of magnesium in the Sd3 sample also explains the presence of magnesioferrite as the final product of siderite decomposition. The presence of Ca is probably the result of the small amount of dolomite in the investigated samples (Figure 1).

Table 2.
The content (%wt) of elements in the initial siderites samples Sd1 and Sd3. The relative uncertainty of the content of individual elements is less than 1 %

C	O	Mg	Al	Si	Ca	Fe	Sum
Sd1							
6.2	48.6	0.8	2.6	4.6	0.9	35.0	98.7
Sd3							
6.3	50.8	3.9	4.1	6.9	0.9	25.5	98.4

Selected Mössbauer spectra of siderite samples heated in an air and a vacuum are presented in Figures 2 and 3. These figures show individual fitted spectra components. Their contributions and hyperfine parameters are presented in Figure 4. The Mössbauer spectra of the initial samples contain a characteristic for siderite ferrous doublet with isomer shift (IS) values of 1.23 and 1.24 mm/s and quadrupole splitting (QS) of 1.80 and 1.81 mm/s for samples Sd1 and Sd3, respectively (Figure 4a). The obtained parameters for siderite are consistent with the literature [13, 14]. Slightly higher IS and QS values for the doublet in the Sd3 sample may indicate the substitution of Fe^{2+} ions by Mg^{2+} in the siderite structure. What is important, one component in the Mössbauer spectrum confirms that all the iron ions in the sample are located in a siderite structure.

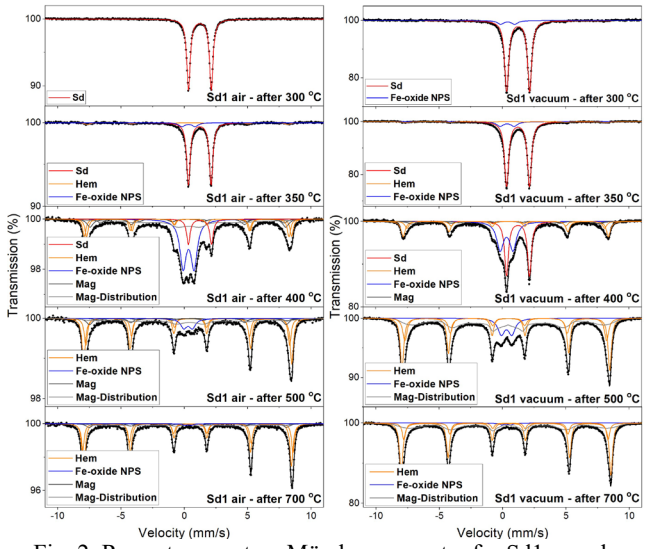

Fig. 2. Room temperature Mössbauer spectra for Sd1 sample heated at selected temperatures in an air and a vacuum. The experimental points, fitting curves and spectral components corresponding to particular iron sites in different phases (colored lines) are presented; Sd – siderite, Mag – magnetite, Hem – hematite, Fe-oxide NPS – Fe-oxide nanoparticles, Mag-Distribution – a sextet representing a hyperfine magnetic field distribution for poorly crystalline magnetite

Heating at temperatures of 300 ºC and 350 ºC does not cause significant changes in the Mössbauer spectra of investigated siderites (Figure 2 and 3), regardless of the atmosphere in which the samples were heated or their type (Sd1 or Sd3). The spectra show a ferrous doublet with hyperfine parameters characteristic of siderite (Figure 4a). However, a ferric doublet appears with a small contribution after heating the samples at 300 ºC. The appearance of a component other than that representing siderite indicates that its decomposition started. This component is probably related to Fe-oxide nanoparticles [15, 16], which is indicated by the values of its hyperfine parameters, such as isomer shift (IS_{NPS}) and quadrupole splitting (QS_{NPS}) (Figure 4b). The contribution of this component is the highest after heating Sd1 sample at 400 ºC and Sd3 at 500 ºC (Figure 4b), and then gradually decreases, which indicates the crystallization of Fe-oxides above this temperature. After heating the Sd1 sample at a temperature of 350 ºC, a sextet associated with hematite is also visible (Figure 2).

Significant changes in the Mössbauer spectra are visible after heating the samples at a temperature of 400 ºC. In the case of sample Sd1, the hematite-related sextet constitutes the main part of the spectrum. This part of the spectrum was matched with two sextets with slightly different values of hyperfine magnetic fields (51 T and 50 T) characterizing this iron oxide. The room temperature Mössbauer spectrum of hematite is represented by one sextet associated with only one crystalline lattice site for Fe^{3+} in hexagonal α-Fe_2O_3 [17]. For this reason, these sextets suggested this iron oxide is probably generated in two different

paths. Also, a sextet with a lower magnetic field indicates some substitution of iron atoms by others like Al or Ti. Apart from the sextets associated with hematite, two other sextets and broad magnetic components fitted using hyperfine magnetic field distribution are visible (Figure 2). These components are associated with iron ions in magnetite, which is well crystallized (sextets) and characterized by low crystallinity (distribution). The processes in the heated Sd1 sample occur similarly in an air and a vacuum, with the difference that they occur slower in a vacuum. What is surprising is the significant amount of hematite in the Sd1 sample heated in a vacuum. The decomposition process in a vacuum seems to proceed in the way proposed below. The siderite decomposition process in a vacuum is described by the equation [18]:

$$3FeCO_3 \rightarrow Fe_3O_4 + 3C + 5/2O_2\,. \quad (1)$$

In the above reaction, oxygen is produced, so the another reaction is possible [18]:

$$4FeCO_3 + O_2 \rightarrow 2Fe_2O_3 + 4CO_2\,. \quad (2)$$

Reaction (2) produces hematite, but only as long as siderite is in the sample. The presence of a weakly crystalline magnetite may also be explained by the reaction proposed below [19]:

$$9Fe_3O_4 + 2O_2 \rightarrow 12Fe_2O_3 + (Fe_3O_4)_{Surface}\,. \quad (3)$$

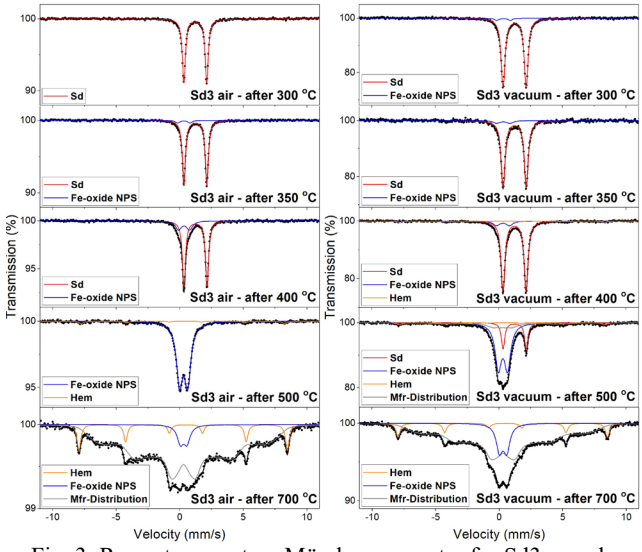

Fig. 3. Room temperature Mössbauer spectra for Sd3 sample heated at selected temperatures in an air atmosphere and in a vacuum. The experimental points, fitting curves and spectral components corresponding to particular iron sites in different phases (colored lines) are presented; Sd – siderite, Hem – hematite, Fe-oxide NPS – Fe-oxide nanoparticles, Mfr-Distribution – a sextet representing a hyperfine magnetic field distribution for poorly crystalline magnesioferrite

Reaction (3) indicate that oxidizing magnetite leads to hematite but magnetite and hematite have different crystal symmetries, from this reason hematite domains must nucleate before they can grow. As was shown [18], the high-temperature oxidation grows magnetite at the surface and hematite in the interior. It means that different reactions occur in the interior (where hematite forms) and at the surface (where new magnetite forms). Equations (2) and (3) also show two paths in which hematite is formed.

In sample Sd3, the decomposition process of siderite occurs much slower than in Sd1. Perhaps the substitution of Fe by Mg in siderite structure results in its greater temperature stability. As in the case of the Sd1 sample, the decomposition process of siderite heated in a vacuum occurs much slower than in an oxygen atmosphere, but the decomposition products are similar regardless of the atmosphere in which the sample was heated. However here, unlike the Sd1 sample, the main decomposition products are Fe-oxide nanoparticles and weakly crystalline magnetioferrite. The formation of magnetioferrite in sample Sd3, and not magnetite as in Sd1, is confirmed by the isomer shift values obtained for these components (Figure 4d) and X-ray diffraction results.

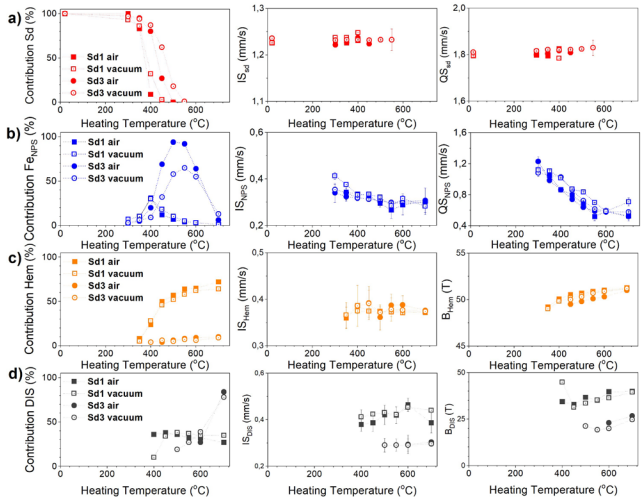

Fig. 4. Contribution of components in Mössbauer spectra and their hyperfine parameters versus heating temperature for siderite (Sd1 and Sd3) (a), Fe-oxide nanoparticles (NPS) (b), hematite Hem (c), DIS – a sextet representing a hyperfine magnetic field distribution for poorly crystalline magnetite (Sd1) or magnesioferrite (Sd3) (d)

The open points characterize the parameters during heating the sample in an air, and the hollow points describe the parameters during the heating of the sample in a vacuum. The lines indicate the trends of the data and act as a guide to the eye.

4. Conclusions

The presented research results show the decomposition process of siderite heated in an oxygen atmosphere and a vacuum. The analysis of phases containing Fe was carried out using Mössbauer spectroscopy. This nuclear method uses the Fe nucleus in our investigated material to probe its local environment. The research results show that the siderite decomposition process will begin at a temperature of approximately 300 °C. For pure $FeCO_3$

complete decomposition occurs after the sample is heated in an air at 450 ºC. This process is extended towards higher temperatures, up to ~500 ºC, for siderite doped mainly by Mg. Moreover, this process occurs slowly for samples heated in a vacuum and shifts towards higher temperatures than for samples heated in an air atmosphere at about 50 ºC. The main products of siderite decomposition are hematite, magnetite or magnesioferrite. However, in the first stage of siderite decomposition, they are nanoparticles of Fe-oxides, and their crystallization process begins in the final stage of siderite decomposition. Moreover, the crystallization process of magnetite is very slow, and even after heating the sample at a temperature of 700 ºC, it constitutes a disordered crystalline phase.

References

[1] Klein, C. (2005). Some precambrian banded iron-formations (biifs) from around the world: their age, geologic setting, mineralogy, metamorphism, geochemistry, and origin. *American Mineralogist.* 90(10), 1473-1499. https://doi.org/10.2138/am.2005.1871.

[2] Cerantola, V., McCammon, C., Kupenko, I., Kantor, I., Marini, C., Wilke, M., Ismailova, L., Solopova, N., Chumakov, A., Pascarelli, S. & Dubrovinsky, L. (2015) High-pressure spectroscopic study of siderite ($FeCO_3$) with a focus on spin crossover. *American Mineralogist*. 100(11-12), 2670-2681. https://doi.org/10.2138/am-2015-5319.

[3] Zhu, X., Han, Y., Sun, Y., Gao, P. & Li, Y. (2022). Thermal decomposition of siderite ore in different flowing atmospheres: phase transformation and magnetism. *Mineral Processing and Extractive Metallurgy Review.* 44(3), 201-208. DOI: 10.1080/08827508.2022.2040498.

[4] Mohamed, A., Al-Afnan, S., Elkatatny, S. & Hussein, I. (2020) Prevention of barite sag in water-based drilling fluids by a urea-based additive for drilling deep formations. *Sustainability*. 12(7), 2719, 1-19. https://doi.org/10.3390/su12072719.

[5] Kruszewski, Ł. & Ciesielczuk, J. (2020). The behaviour of siderite rocks in an experimental imitation of pyrometamorphic processes in coal-waste fires: upper and lower silesian case, Poland. *Minerals*. 10(7), 586, 1-23. https://doi.org/10.3390/min10070586.

[6] Ordoñez, L., Vogel, H., Sebag, D., Ariztegui, D., Adatte, T., Russell, J., Kallmeyer, J., Vuillemin, A., Friese, A., Crowe, S., Bauer, K., Simister, R., Henny, C., Nomosatryo, S. & Bijaksana, S. (2019). Empowering conventional Rock-Eval pyrolysis for organic matter characterization of the siderite-rich sediments of Lake Towuti (Indonesia) using End-Member Analysis. *Organic Geochemistry*. 134, 32-44. DOI: 10.1016/j.orggeochem.2019.05.002.

[7] Ponomar, V.P., Dudchenko, N.O. & Brik, A.B. (2017). Phase transformations of siderite ore by the thermomagnetic analysis data. *Journal of Magnetism and Magnetic Materials*. 423, 373-378. DOI: 10.1016/j.jmmm.2016.09.124.

[8] Isambert, A., Valet, J., Gloter, A. & Guyot, F. (2003). Stable Mn-magnetite derived from Mn-siderite by heating in air. *Journal of Geophysical Research: Solid Earth.* 108(B6), 2283, 1-9. DOI: 10.1029/2002JB002099.

[9] Luo, Y.H., Zhu, D.Q., Pan, J. & Zhou, X.L. (2016) Thermal decomposition behaviour and kinetics of Xinjiang siderite ore. *Mineral Processing and Extractive Metallurgy.* 125(1), 17-25. DOI: 10.1080/03719553.2015.1118213.

[10] Rancourt, D.G. & Ping, J.P. (1991). Voigt-based methods for arbitrary-shape static hyperfine parameter distributions in Mössbauer spectroscopy. *Nuclear Instruments and Methods in Physics Research Section B: Beam Interactions with Materials and Atoms.* 58(1), 85-97. DOI: 10.1016/0168-583X(91)95681-3.

[11] Piazzi, M., Morana, M., Coïsson, M., Marone, F., Campione, M., Bindi, L., Jones, A., Ferrara, E. & Alvaro, M. (2019). Multi-analytical characterization of Fe-rich magnetic inclusions in diamonds. *Diamond and Related Materials.* 98, 107489, 1-9. DOI: 10.1016/j.diamond.2019.107489.

[12] Leon-Reina, L., Garcia-Mate, M., Alvarez-Pinazo, G., Santacruz, I., Vallcorba, O., De la Torre, G. & Aranda, M. (2016) Accuracy in Rietveld quantitative phase analysis: a comparative study of strictly monochromatic Mo and Cu radiations. *Journal of Applied Crystallography.* 49, 722-735. DOI: 10.1107/S1600576716003873.

[13] Dhupe, A. & Gokarn, A. (1990). Studies in the thermal decomposition of natural siderites in the presence of air. *International Journal of Mineral Processing*. 28(3-4), 209-220. DOI: 10.1016/0301-7516(90)90043-X.

[14] Ristić, M., Krehula, S., Reissner, M. & Musić, S. (2017). ^{57}Fe Mössbauer, XRD, FT-IR, FE SEM Analyses of Natural Goethite, Hematite and Siderite. *Croatica Chemica Acta*. 90(3), 499-507. DOI: 10.5562/cca3233.

[15] Klekotka, U., Winska, E., Satuła, D. & Kalska-Szostko, B. (2018). Mössbauer studies of surface modified magnetite particles. *Acta Physica Polonica A.* 134(5), 1003-1006. DOI: 10.12693/APhysPolA.134.1003.

[16] Gervits, N., Gippius, A., Tkachev, A., Demikhov, E., Starchikov, S., Lyubutin, I., Vasiliev, A., Chekhonin, V., Abakumov, M., Semkina, M. & Mazhuga, A. (2019). Magnetic properties of biofunctionalized iron oxide nanoparticles as magnetic resonance imaging contrast agents. *Beilstein Journal of Nanotechnology.* 10(1), 1964-1972. DOI: 10.3762/bjnano.10.193.

[17] Lyubutin, I., Lin, C., Korzhetskiy, Yu., Dmitrieva, T. & Chiang, R. (2009). Mössbauer spectroscopy and magnetic properties of hematite/magnetite nanocomposites. *Journal of Applied Physics.* 106(3), 034311. DOI: 10.1063/1.3194316.

[18] Mendoza, E., Santos, A., Lopez, E., Drozd, V. & Durygin, A. (2019). Iron oxides as efficient sorbents for CO_2 capture. *Journal of Materials Research and Technology*. 8(3), 2944-2956. DOI: 10.1016/j.jmrt.2019.05.002.

[19] McCarty, K., Monti, M., Nie, S., Siegel, D., Starodub, E., El Gabaly, F., McDaniel, A., Shavorskiy, A., Tyliszczak, T., Bluhm, H., Bartelt, N. & de la Figuera, J. (2014). Oxidation of magnetite(100) to hematite observed by in situ spectroscopy and microscopy. *The Journal of Physical Chemistry C*. 118(34), 19768-19777. DOI: 10.1021/jp5037603.